Table of content

Supplementary methods

SB1 expression analysis of YAP, CK-7, and CK-19 proteins

Western blots were performed to determine the expression of YAP, CK-7, and CK-19, known to be highly expressed in CCA. Whole cell lysates were added by adding ice cold lysis buffer (Mammalian Protein Extract Reagent [1]) containing protease inhibitors (Halt Protease and Phosphatase Inhibitor, Thermo Fisher Scientific). The lysed cells were then centrifuged, and supernatant was collected. Protein concentration was determined by the Pierce BCA Protein Assay (Thermo Fisher Scientific). Proteins were then resolved by SDS-PAGE electrophoresis and transferred to PVDF membranes. Membranes were blotted with primary antibodies at 4°C overnight in 5% non-fat milk in TBS Tween. The primary antibody dilution was 1:1000 unless otherwise indicated. The following primary antibodies were used for immunoblot analysis: YAP (sc-101199 - Santa Cruz Biotechnology), CK-7 (clone ERP17078, abcam) and CK-19 (clone EP1580Y- abcam), b-Actin (clone 622101, BioLegend). After overnight incubation, membranes were washed for 15 minutes in PBS-Tween and then horseradish peroxidase conjugate secondary anti-mouse antibodies (Cell Signaling Technology), rabbit (Cell Signaling Technology) and rat (BioLegend) were added to membrane at a concentration of 1:2000 and incubated for 1 hour at room temperature. Immunoblots were visualized with enhanced chemiluminescence reagents (Clarity/Clarity Max ECL BioRad).

YAP/AKT and NOTCH/AKT iCCA tumor model

Eight-week-old female C57BL/6 underwent hydrodynamic tail vein injections (HDTVinj) with 20μg of AKT, 30μg of YAP and 2μg of HSB2 plasmids (or 4μg AKT, 20 μg NICD (activated NOTCH) and 1μg HSB2) dissolved in a total volume of 1600μl PBS as previously described[2].

YAP, AKT, NICD and HSB2 plasmids were grown in E. coli cultures and isolated using a Plasmid DNA Maxiprep Kit. Plasmid concentrations were measured using a NanoDrop Spectrophotometer™. Mice were shown to have microscopic tumor lesions as early as 3 weeks and these lesions were confirmed to be CCA based on CK-19 staining (Suppl. Fig. 2). Treatment was therefore initiated at 21 days with either bi-weekly IgG Control (alternating 1ug/g and 0.5ug/g) (days, 24, 26, 31, 33, 38, 40, 45, 47 post plasmid injection) (n=8), weekly anti-PD-1 (1ug/g) (days 26, 33, 40, 47 post plasmid injection) (n=8), weekly anti-CD40 (0.5ug/g) (days 24, 31, 38, and 45 post plasmid injection) (n=8), or combination anti-CD40+anti-PD-1 (n=8) with the treatment schedule as above. Mice were euthanized at day 49. Mice and livers were weighed by a blinded observer. Representative liver tissue sections from each mouse was fixed in 4% paraformaldehyde (Fisher Scientific, Hampton, New Hampshire, USA) overnight and transferred into 70% ethanol prior to paraffin-embedding. Hematoxylin and eosin stained sections were scanned at 20× objective magnification (0.5 μm/pixel) using an Aperio AT2 digital whole slide scanner (Leica Biosystems, Buffalo Grove, IL). Presence of CCA and extent of tissue infiltration was confirmed by an experienced murine histopathologist. Automated quantification of tumor areas and normal liver tissue areas was performed using HALO™ image analysis software (Indica Labs, Corrales (NM), USA). Unique algorithms were applied using the pattern recognition image analysis integrated software (i.e. supervised machine learning - *Random Forest classifier*). Blood was drawn from mice from each group and spun down (n=5 per group). Serum was sent to our institution's biochemistry laboratory and analyzed for liver function tests (alanine and aspartate aminotransferases (ALT and AST, respectively)) to detect any treatment associated hepatic toxicity.

Murine Immunohistochemistry

Tumor bearing mouse livers were excised 28 days after SB1 tumor cell inoculation. Livers were fixed in 4% PFA. H&E was performed to characterize tumor architecture. IHC analysis of these liver samples included staining for macrophages (Iba1 – Biocare), dendritic cells (CD11c – Cell Signaling), CD4 T Cells (CD4 -eBioscience), CD8 T Cells (CD8a - eBioscience), PD-1 (R&D Systems), PD-L1 (R&D Systems), CD40 (abcam). Positive tissue staining for the above antibodies was programmed into the HALO™ image analysis software (Indica Labs, Corrales (NM), USA). Cell positivity was then quantified in cells per mm2 of tissue.

Human tissue microarray and immunohistochemistry

To confirm the findings noted in mice, human samples were stained for CD40. A tissue microarray (TMA) containing human intrahepatic CCA samples and corresponding non-tumorous liver tissue (n=49 patients)[3]. All patients received a liver resection at the University Hospital RWTH Aachen, Germany and informed consent for this retrospective study was not required (ethics vote EK 122/16). IHC was performed on 5µm sections. CD40 IHC was performed (clone B-B20, Cymbus Biotechnology). Staining was assessed on tumor cells, macrophages, Kupffer cells, and lymphocytes.

Cohort and OS prediction

A set of 130 surgical paired tumors and nontumor specimens of iCCA patients from the TIGER-LC cohort[4] (Thailand) was used in this study. Mixed HCC and ICC samples were excluded from analysis. Transcriptomic and survival information were available for 57 iCCA patients (n=28 low expression and n=29 for high expression) for paired tumor and non-tumor tissue. R Studio (version 1.2.5, R Foundation for Statistical Computing, Austria, package “survival“) and GraphPad Prism

Software (version 8.3.0, USA) were used for OS analysis of the TIGER Cohort (Asian CCA cohort). Survival risk prediction was performed based on CD40 expression in the tumor tissue. Kaplan-Meier survival curves were provided with two risk groups (high versus low, where high was defined as the upper third of CD40 and low as the bottom third of CD40, respectively). Statistical significance was calculated based on log-rank test. A p-value below 0.05 was considered significant.

Flow cytometry

Liver infiltering mononuclear cells were prepared as previously reported [5]. Briefly, livers were removed immediately after mice were sacrificed. After homogenization, debris was removed by filtering samples through nylon mesh. Liver infiltrating cells were isolated by isotonic Percoll centrifugation (850xg, 25min). Red blood cells were lysed by using ACK lysing buffer. Cells were surface-labeled with indicated antibodies for 30 minutes at 4ºC. Intracellular staining using a Foxp3/transcription factor staining buffer set (eBioscience) was used according the manufacturer's instructions. Flow cytometry was performed on CytoFLEX LX platforms and results were analyzed using FlowJo software version 10.4.2 (TreeStar Inc). Dead cells were excluded by using live/dead fixable near-IR dead cell staining kit (ThermoFisher scientific). The following antibodies were used for flow cytometry analysis: anti-CD3 BV605 (clone 17A2, Biolegend), anti-CD4-FITC (clone RM4-5, Biolegend), anti-CD8-Alexa Fluor 700 (clone 53-6.7, Biolegend), anti-NK1.1-BV510 (clone PK-136, Biolegend), anti-CD69-BV421 (clone H1.2F3, Biolegend), anti-OX40-PE (clone OX-86, Biolegend), anti-CD44-PE/Cy7 (clone 1M7, Biolegend), anti-CD62L PerCP/Cy5 (clone MEL-14, Biolegend), anti-Tim3-BV421 (clone RMT3-23, Biolegend), anti-CD3 PerCP/Cy5.5 (clone 17A2, Biolegend), anti-CD4-PE/CY7 (clone GK1.5, Biolegend), anti-PD1-

FITC (clone 29F.1A12, Biolegend), anti-LAG3-APC (clone C9B7W, Biolegend), anti-CD69-Alexa Fluor 700 (clone H1.2F3, Biolegend), anti-FOXP3-APC (clone FJK-16s, eBioscience), anti-T-bet-PE/Cy7 (clone 4B10, Biolegend), anti-GATA3-PerCP/Cy5 (clone 16E10A23, Biolegend), anti-RORgt-PE (clone B20, eBioscience), anti-CD4-Alexa Fluor 700 (clone GK1.5, Biolegend), anti-CD8-BV421 (clone 53-6.7, Biolegend), anti-IFN-γ-APC (clone XMG1.2, Biolegend), anti-CD11b-PB (clone M1/70, Biolegend), anti-CD11c-BV650 (clone N418, Biolegend), anti-F4/80-PE (clone BM8, eBioscience), anti-CD40-FITC (clone 3/23, Biolegend), anti-MHCII(I-A-I-E)-BV510 (Biolegend M5/114.15.2, Biolegend), anti-CD86-APC (clone GL-1, Biolegend).

Clustering analysis and t-SNE visualization

Clustering analysis was performed in order to analyze and visualize the high-dimensional nature of our flow cytometry data. First, we applied FSC-A/SSC-A and gated for Live/Dead cells. We then applied CD3, NK1.1, CD8, and CD4 gates. For activation, we selected $CD3^-/NK1.1^+$, $CD3^+/CD4^+$, and $CD3^+/CD8^+$ and gated for frequency of $CD69^+$ and $OX40^+$. We then randomly sampled 50,000 cells from the final gate per animal for our analysis and used a t-distributed stochastic neighbor embedding (t-SNE) Barnes-hut algorithm to reduce the dimensionality of the data set for visualization. In order to cluster the data appropriately, a network graph was created using k-nearest neighbors (k ¼ 60), and a clustering solution was solved for by maximizing the modularity of the graph. All visualizations of clustering were through the use of t-SNE heat maps.

Depletion Experiments

Eight-week-old C57BL/6 mice underwent orthotopic SB1 tumor cell injection and treatment as described above. In addition, 3 separate depletion experiments were performed. A first cohort received bi-weekly clodronate liposomes vs control liposomes (on days -2, 2, 5, 8, 12, 15, 19, 22

and 26 post orthotopic injections) in addition to treatment as described above. A second cohort received weekly anti-CD4 vs IgG control (on days -2, 5, 12, 19, 26 post orthotopic injections) in addition to treatment as described above. A final cohort received weekly anti-CD8 vs IgG control (on days -2, 5, 12, 19, 26 post orthotopic injections) in addition to treatment as described above. In all 3 experiments, mice were euthanized at day 28. Livers and tumors were weighed and tumor to liver weight ratios were calculated and compared between groups. Measurements were performed by a blinded observer.

Response to Gem/Cis vs anti-CD40+anti-PD-1 in orthotopic and advanced subcutaneous tumors

SB1 orthotopic tumor were induced as described above. Mice were treated with weekly intraperitoneal (i.p) gemcitabine (100 mg/kg) and cisplatin (4mg/kg) in 100uL of PBS (n=8). A second group was treated anti-CD40+anti-PD-1 as described above (n=8). Control mice were treated with i.p PBS with IgG2 as described above (n=8). Mice were sacrificed on day 28. Mice were weighed and groups were compared for treatment tolerability. Tumors and livers were weighed and tumor to liver ratios were calculated as above. To assess differences in long term survival and treatment efficacy for advanced disease, C57BL/6 mice underwent SB1 subcutaneous injections. When the tumors reached 10mm in size, mice were started on treatment with Gemcitabine/Cisplatin alone (n=7), Gemcitabine/Cisplatin+anti-CD40+anti-PD-1 (n=7) or IgG2 Control in PBS (n=7). Tumor size was measured by caliper as greatest diameter and mice were sacrificed when tumors reached 20mm in diameter or tumor necrosis exceeded 50% of the tumor surface. Mouse survival was calculated as the time from inoculation to euthanasia mandated by

tumor reaching the above thresholds. Measurements for all the above experiments were performed by a blinded observer.

CD107 degranulation assay

Splenocytes were isolated from mice and 1 x 10^6 cells/well were mixed with anti-CD107a-PE (1:500, clone 1D4B, BD Biosciences) and incubated with or without SB1 tumor cells (5 x 10^4 cells/well) in a 96-well round bottom plate with Menensin in RPMI supplemented with 10% FBS. Cells were incubated at 37°C for 5 hr, then were washed and stained with cell surface markers. Cells were fixed and permeabilized using a Cytofix/Cytoperm kit (BD biosciences) followed by intracellular cytokine detection with anti-IFNγ-PE/Cy7 (1:100) in permeabilization buffer for 30 min at 4°C. Cells were washed and analyzed as mentioned above for IFNγ and CD107a expression on $CD8^+$ T cells was determined. Tumor specific degranulation was measured by subtracting $CD107^+$ % $CD8^+$ T cells $_{\text{(no SB1 tumor cell incubation)}}$ from $CD107^+$ % $CD8^+$ T cells $_{\text{(incubated with SB1 tumor cells)}}$.

References

1. Rizvi, S., et al., *YAP-associated chromosomal instability and cholangiocarcinoma in mice.* Oncotarget, 2018. **9**(5): p. 5892-5905.
2. Yamamoto, M., et al., *Oncogenic Determination of a Broad Spectrum of Phenotypes of Hepatocyte-Derived Mouse Liver Tumors.* Am J Pathol, 2017. **187**(12): p. 2711-2725.
3. Longerich, T., et al., *Factors of transforming growth factor beta signalling are co-regulated in human hepatocellular carcinoma.* Virchows Arch, 2004. **445**(6): p. 589-96.
4. Chaisaingmongkol, J., et al., *Common Molecular Subtypes Among Asian Hepatocellular Carcinoma and Cholangiocarcinoma.* Cancer Cell, 2017. **32**(1): p. 57-70.e3.
5. Kapanadze, T., et al., *Regulation of accumulation and function of myeloid derived suppressor cells in different murine models of hepatocellular carcinoma.* J Hepatol, 2013. **59**(5): p. 1007-13.

Fig. S1

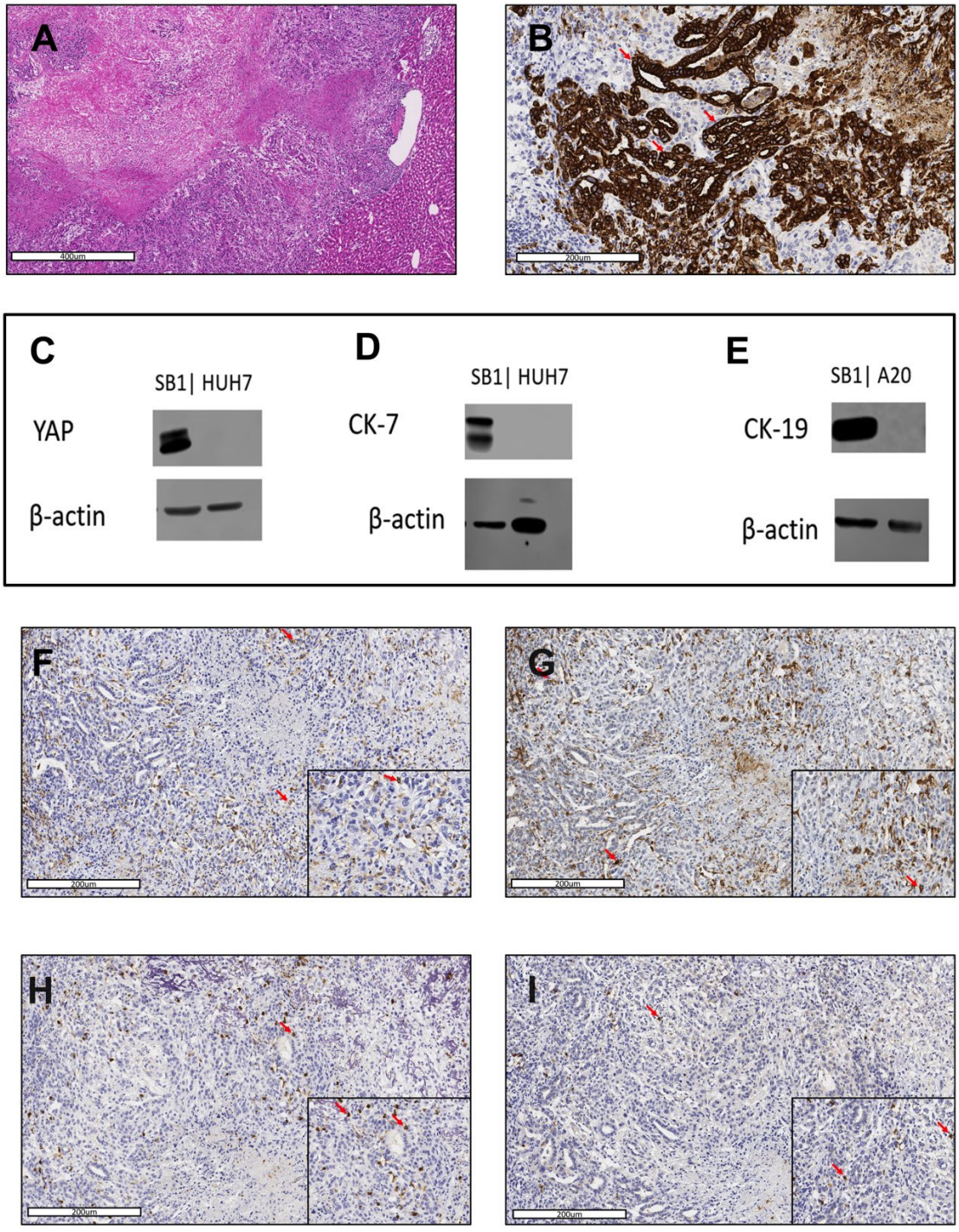

Characterization of the immune infiltrate in SB1 tumors by IHC and Western Blot analysis of SB1 cells

(A)Representative H&E and (B)CK-19 staining of orthotopic SB1 tumor.
(C-E) Western Blot analysis for YAP, CK-7 and CK-19 expression in SB1 cells.
(F-I) Representative IHC staining for tumor infiltrating macrophages (Iba1, F), DCs (CD11c, G), CD4 (H) and CD8 T cells (I).

Fig. S2

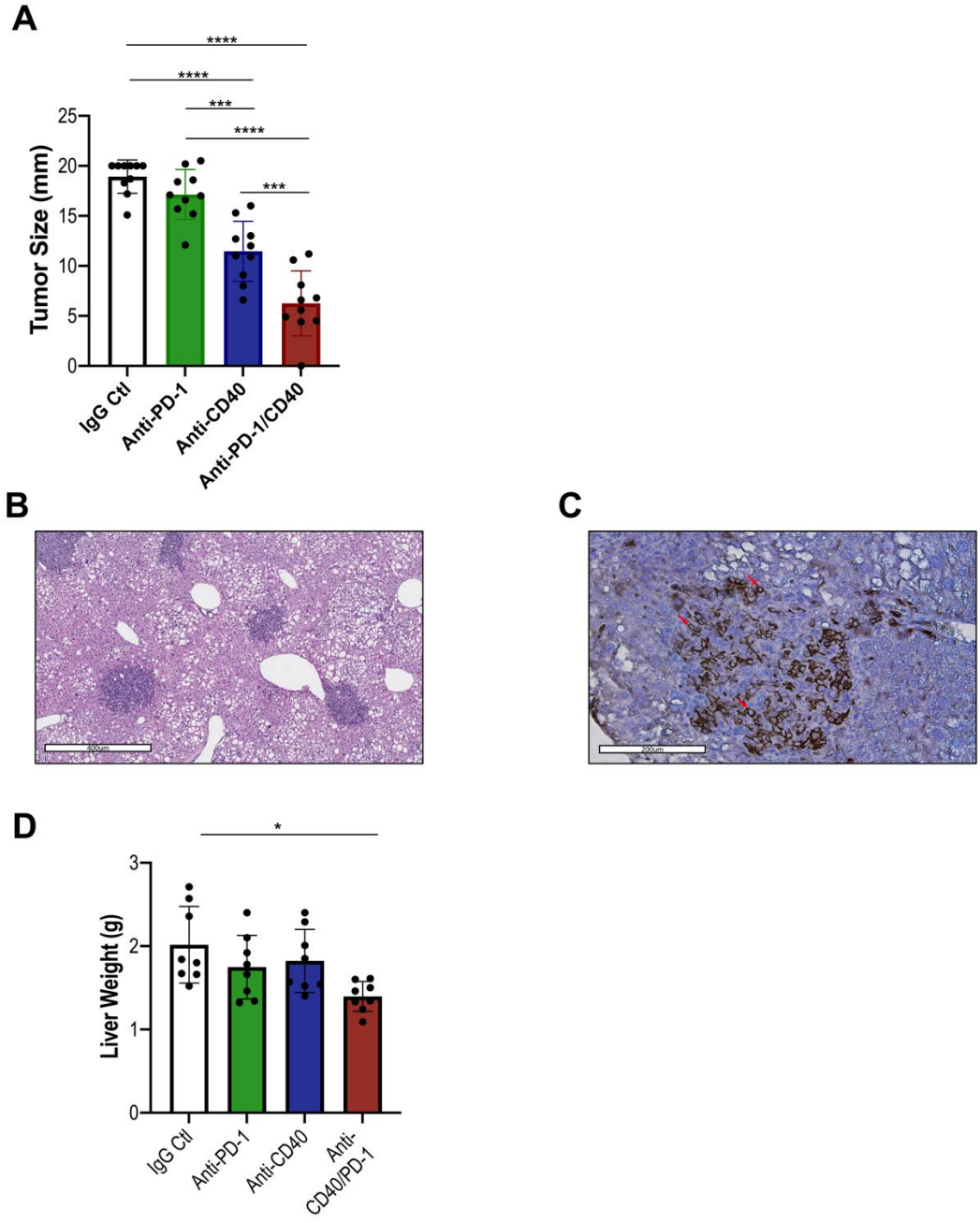

Additional evaluations of response to anti-PD-1, anti-CD40, and anti-CD40+anti-PD-1 (anti-CD40/PD-1) in subcutaneous and YAP+AKT CCA models.
(A) Flank tumor sizes at 4 weeks in mice injected subcutaneously with SB1 and treated with the above treatment regimens (n=10 per group).
(B) HE analysis of iCCA after injection with YAP + AKT
(C) IHC staining for CK19
(D) Liver weights from YAP+AKT derived CCA mice treated with the above treatment regimens (n=8 per group). (one-way ANOVA, *p<0.05; **p<0.01; ***p<0.001; ****p<0.0001)

Fig. S3

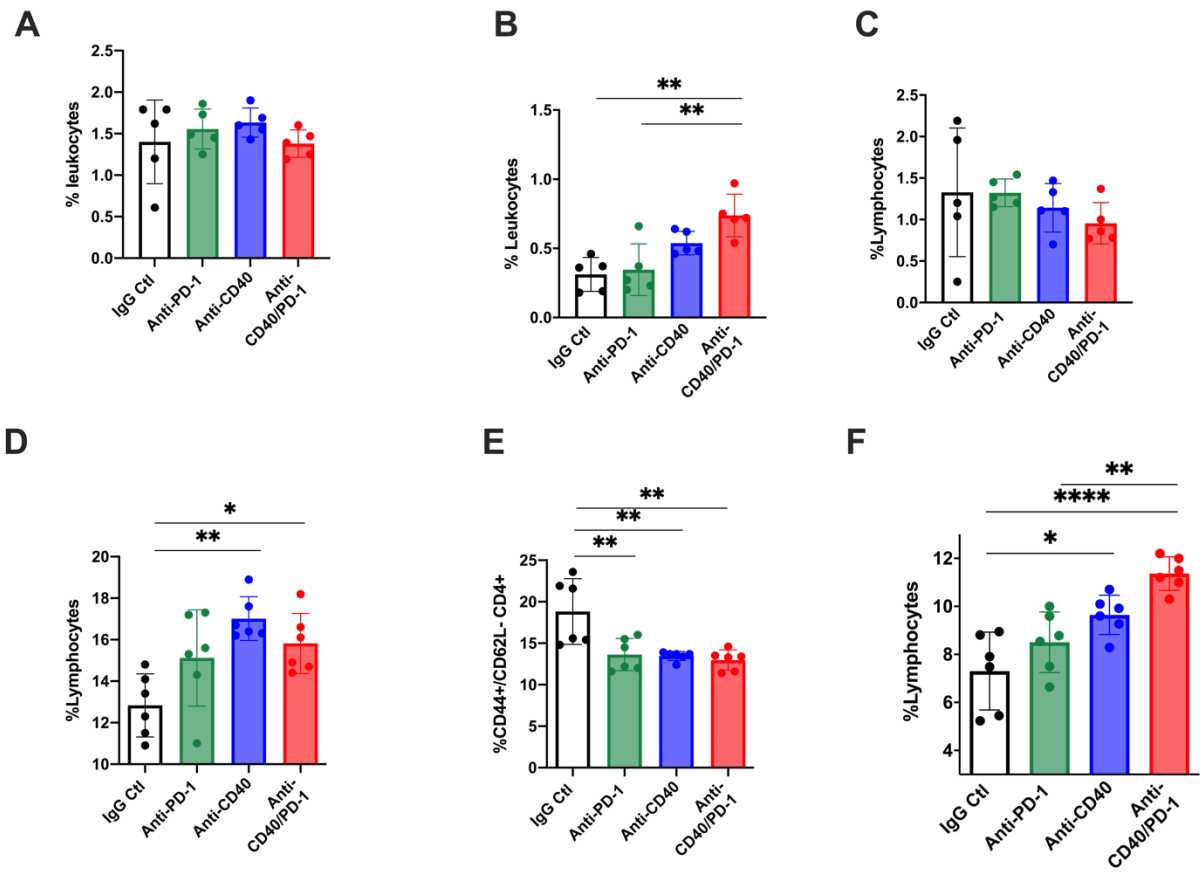

FACS analysis of immune cell populations in spleens of tumor bearing mice treated with anti-PD-1, anti-CD40, or anti-CD40/PD-1. Frequency of **(A)** macrophages ($CD11b^+/F4/80^+$), **(B)** DCs ($CD11C^+$), **(C)** NK cells ($CD3^-NK1.1^+$), **(D)** $CD4^+$ T cells, **(E)** effector memory ($CD44^+/CD62L^-/CD4^+$) T cells, and **(F)** $CD8^+$ T cells (n=6 per group for CD4, effector memory, and CD8 cell analysis. n=5 per group for macrophage, DC and NK analysis). (one-way ANOVA, *p<0.05; **p<0.01; ***p<0.001; ****p<0.0001)

Fig. S4

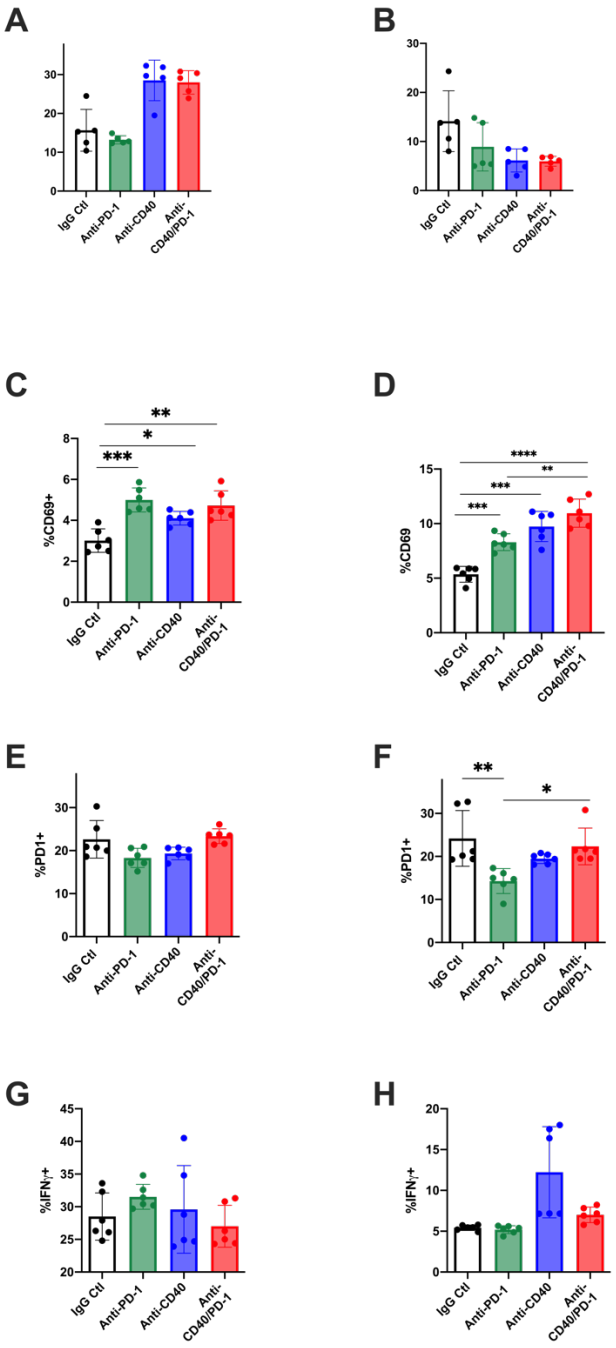

FACS analysis of immune cell activation among hepatic lymphocytes of tumor bearing mice treated with anti-PD-1, anti-CD40, or anti-CD40/PD-1. Frequency of **(A)** $CD86^+$ macrophages ($CD11b^+/F4/80^+$), **(B)** $MHCII^+$ DCs ($CD11C^+$), **(C)** $CD69^+$ $CD8^+$ T cells **(D)** $CD69^+$ NK ($CD3^-/NK1.1^+$) cells **(E)** PD-1^+ $CD8^+$ T cells **(F)** PD-1^+ $CD4^+$ T cells **(G)** IFN-γ^+CD8^+ T cells and **(H)** IFN-γ^+CD4^+ T cells . (n=6 per group for CD4, effector memory, and CD8 cell analysis. n=5 per group for macrophage, DC and NK analysis. (one-way ANOVA, *p<0.05; **p<0.01; ***p<0.001; ****p<0.0001)

Fig. S5

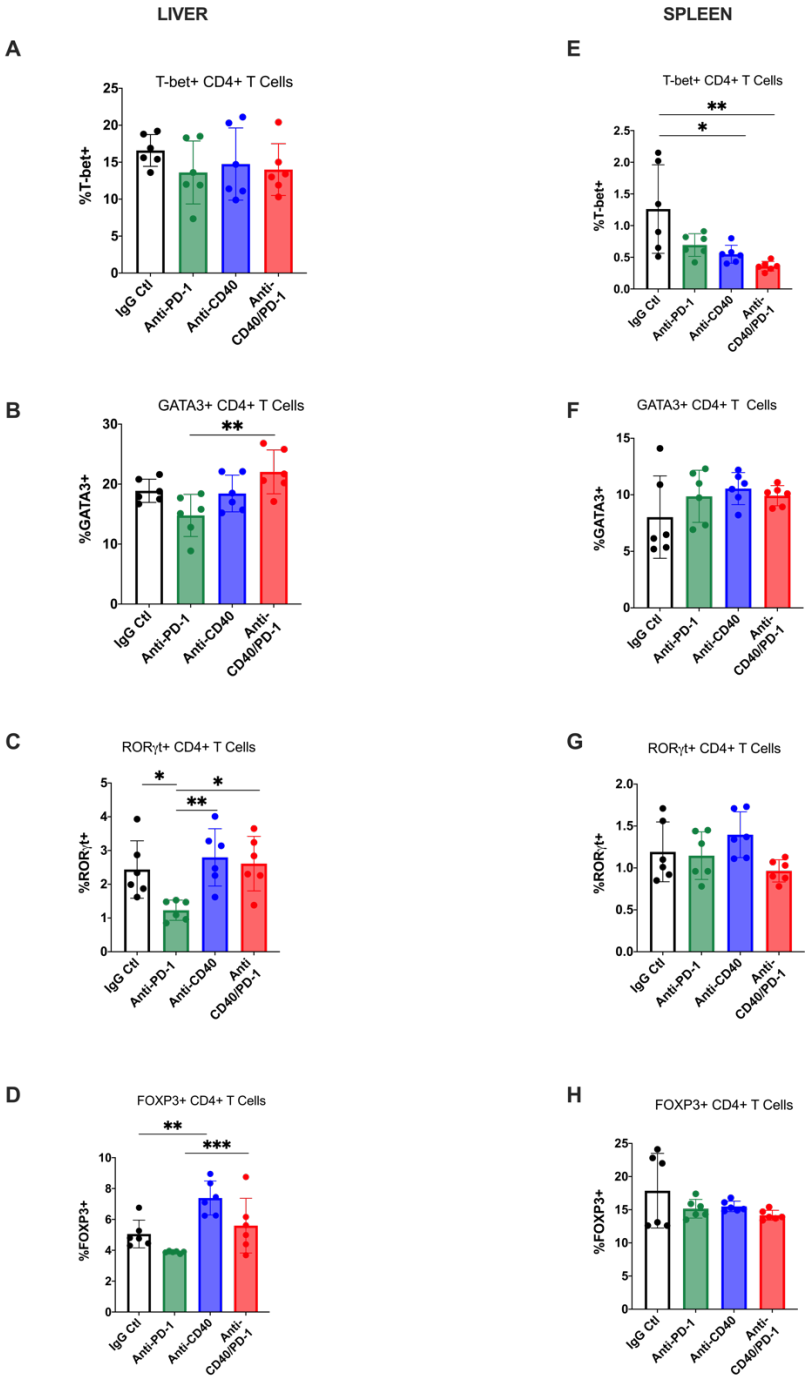

FACS analysis of CD4$^+$ T cell sub-populations (A-D) hepatic lymphocytes and splenocytes (E-H) from YAP+AKT CCA tumor bearing mice treated with IgG Ctl, anti-PD-1, anti-CD40, or anti-CD40+anti-PD-1 (anti-CD40/PD-1). Frequency of Th1 (T-bet$^+$) CD4$^+$ T cells (**A**&**E**), Th2 (GATA3$^+$) CD4$^+$ T (**B**&**F**), Th17 (RORγT$^+$) CD4$^+$ T (**C**&**G**), and helper (FOXP3$^+$) CD4$^+$ T (**D**&**H**) cells among hepatic lymphocytes and splenocytes (n=6 animals per group), respectively. (one-way ANOVA, *p<0.05; **p<0.01; ***p<0.001; ****p<0.0001)

Fig. S6

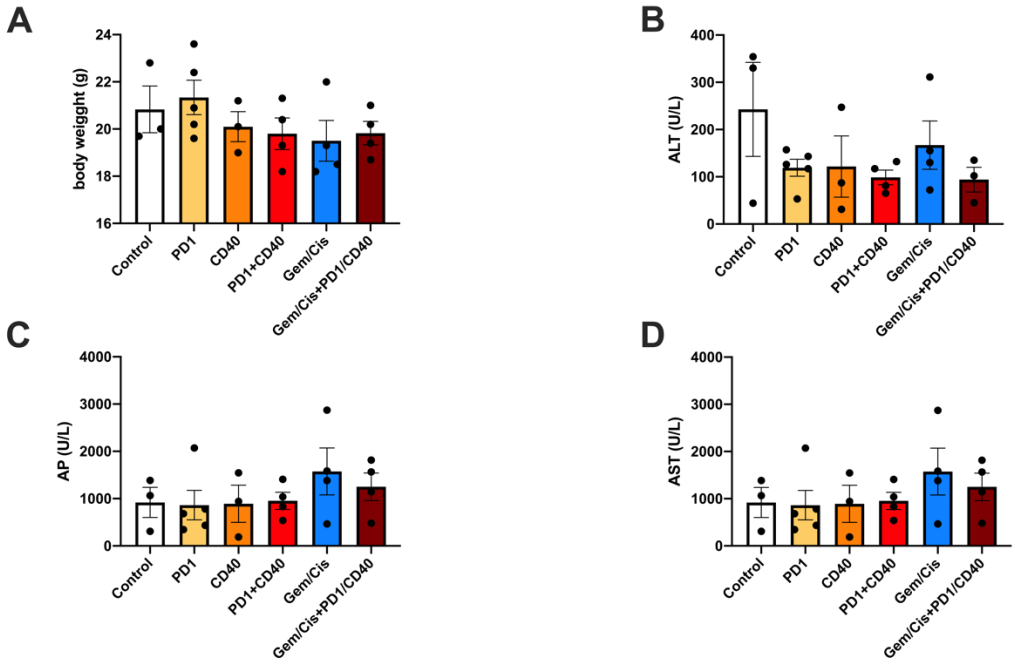

Effects and tolerability of treatment regimens on mouse health. (A) Weights of mice treated with IgG Ctl, anti-PD-1, anti-CD40, or anti-CD40+anti-PD-1 (anti-CD40/PD-1), Gem/Cis or Gem/Cis+PD-1/CD40 at 4 weeks post treatment initiation (n=3-5 per group). Liver function tests including **(B)** ALT and **(C)** AP and **(D)** AST of YAP+AKT CCA C57BL/6 tumor bearing mice compared between treatment groups (n=3-5 per group).